HDPE/hydroxyapatite/zeolite composite – characterization and *in vitro* cytotoxicity

Anandha Moorthy Appusamy[1), *)] (ORCID ID: 0000-0001-5540-8941), **Senthil Kumar Kallippatti Lakshmanan**[1)] (0000-0001-8309-0002), **Balaji Ayyanar Chinnappan**[2)] (0000-0002-2044-4683), **Madheswaran Subramaniyan**[1)] (0000-0001-7106-7104)

DOI: https://doi.org/10.14314/polimery.2024.9.4

Abstract: The HDPE/HA/zeolite (65/30/5) composite was obtained by injection molding. Hydroxyapatite (HA) was synthetized using microwave technique. FT-IR showed the presence of hydroxyl and phosphate functional groups. The structure was studied using X-ray diffraction (XRD), and field emission scanning electron microscope (FESEM). The energy dispersive X-ray analysis (EDAX) revealed the presence of O, Ca, P, C, Na, Cl, and Mg. The composite showed improved tensile strength, compressive strength and hardness compared to pure HDPE. *In vitro* cytotoxicity studies were conducted using L929 cells line. The tests showed 94% viability and 6% toxicity of cells.

Keywords: HA, zeolite, HDPE, L929 cells, cytotoxicity.

Kompozyt HDPE/hydroksyapatyt/zeolit – charakterystyka i cytotoksyczność *in vitro*

Streszczenie: Metodą formowania wtryskowego otrzymano kompozyt HDPE/HA/zeolit (65/30/5). Hydroksyapatyt (HA) otrzymano techniką mikrofalową. Badania FT-IR wykazały obecność grup funkcyjnych hydroksylowych i fosforanowych. Strukturę badano za pomocą dyfrakcji rentgenowskiej (XRD) i skaningowego mikroskopu elektronowego z emisją polową (FESEM). Analiza rentgenowska z dyspersją energii (EDAX) wykazała obecność O, Ca, P, C, Na, Cl i Mg. Kompozyt wykazał wi**ęks**zą wytrzymałość na rozciąganie, wytrzymałość na ściskanie i twardość w porównaniu z czystym HDPE. Badania cytotoksyczności *in vitro* przeprowadzono przy użyciu linii komórkowej L929. Testy wykazały 94% żywotności i 6% toksyczności komórek.

Słowa kluczowe: HA, zeolit, HDPE, komórki L929, cytotoksyczność.

Metals and alloys are usually used in bone implants because they have suitable mechanical properties and load-bearing capacity. Implants with high modulus cause stress shielding and there is also a serious risk that they may leak toxic ions into the environment. To solve this problem and improve bone properties such as osteoinduction and osteoconduction, the metal surface of implants is coated with various materials [1–5]. The most common coating materials are hydroxyapatite (HA) and calcium phosphate. Hydroxyapatite is studied in detail as a coating material for metal implants because it contains bone-like elements such as Li^+, K^+, Na^+, Mg^{2+}, Sr^{2+}, Zn^{2+}, etc. [6–10]. Among several minerals studied, a substitute for hydroxyapatite for zinc and magnesium has been obtained using microwave irradiation technique and investigated [11–14]. Zinc (Zn) is a key metal that has been implicated in the study of biochemistry in bone tissue engineering. It appears to be the most abundant trace metal element discovered in bone and a potential candidate for bone formation stimulator [15].

It was believed that acclimation of Zn to HA-coated grafts could stimulate bone formation around the material [16]. The essential trace element Zn has a stimulating effect on bone metabolism in the human body [17]. In addition, Zn is considered as a potential substitute due to its biological importance [18]. Current research is focused on improving properties of hydroxyapatite by adding magnesium (Mg) and zinc (Zn) to its structure, because these elements are essential for the early stages of osteogenesis and have a stimulating effect on bone metabolism [19]. Furthermore, zeolite was added to improve the biological properties due to its porous nature. In addition to metals and ceramics, polymers are used as bone substitutes. Both natural and synthetic polymeric materials are widely used in bone tissue engineering. To date, many

[1)] Department of Mechanical Engineering, Bannari Amman Institute of Technology, 638401 Erode, India.

[2)] Department of Mechanical Engineering, Coimbatore Institute of Technology, Coimbatore, 641014 Tamilnadu, India.

[*)] Author for correspondence:
anandhamoorthya@bitsathy.ac.in

polymers have been identified as scaffolds for bone regeneration, including polylactic acid (PLA), polyglycolic acid (PGA), polycaprolactone (PCL), and polymethyl methacrylate (PMMA). Polyethylene (PE) is a promising material due to its high strength, flexibility, cost-effectiveness, and biocompatibility [20]. Furthermore, high-density polyethylene-hydroxyapatite composites have been used as a bone substitute material in clinical applications, including orbital floor prostheses and middle ear implants [21-25]. This combination represents the lower limit for cortical bone, as it has the high stiffness, brittleness, and low mechanical properties of hydroxyapatite and the low modulus combined with the strength of high-density polyethylene (HDPE). To date, reinforced HA composites have been obtained using a variety of materials [26, 27].

Zeolites are promising minerals due to their high compatibility with hydroxyapatite and their unique properties. Therefore, the combination of HA and zeolite is expected to improve the properties of HDPE. The reason for choosing the matrix and reinforcements is calcium-rich compounds, which are readily available in human bones, have high intermolecular strength, high tensile strength, and high specific strength. The main objective of this study was to develop novel HA/zeolite/HDPE composites and conduct an *in vitro* study of their structure and functional properties. The composites obtained by injection molding [20] were subjected to comprehensive analysis in terms of structure, mechanical, thermal, and biological properties.

EXPERIMENTAL PART

Materials

HDPE (Sun Polymers, Coimbatore, India) with a density of 0.954 g/cm^3 and thermal conductivity of 0.29 W/mk was used as the matrix. HA was synthesized by microwave irradiation according to the procedure published elsewhere [20, 26]. Briefly, disodium hydrogen phosphate, calcium nitrate tetrahydrate and ethylenediaminetetraacetic acid were used to obtain HA, maintaining the calcium to phosphorus ratio at 1.67 [27]. Zeolite with a bulk density of 0.8 g/cm^3 was purchased from Sigma-Aldrich. The chemicals used in this study are listed in Table 1.

Composite preparation

The HDPE composite (65 wt%) with the addition of HA (30 wt%) and zeolite (5 wt%) was obtained using an injection molding machine, maintaining a temperature of 135°C and a pressure of 50 bar.

Methods

Fourier infrared spectroscopy (FT-IR) analysis was performed by using a Bruker Alpha spectrometer (Billerica, MA, USA), the spectra were recorded using at least 64 scans with 2 cm^{-1} resolution, in the spectral range 4000–500 cm^{-1}, using KBr pellets technique with ZnSe for humidity control. X-ray diffraction (XRD) measurements were performed on the Bruker diffractometer (Billerica, MA, USA) using Cu K radiation (1.54 °A) with 50 kV and 40 mA. The crystallites size was calculated using the Debye–Scherrer equation (1).

$$D = K\lambda/\beta\cos\theta \quad (1)$$

where: D – mean grain size, K – dimensionless shape factor (0.92), λ – X-ray wavelength (1.5418 Å), β – the line broadening at half the maximum intensity (0.174533 rad), θ – Bragg angle (11.5°).

The morphology and elemental composition of the samples were studied using FESEM (Carl Zeiss, Oberkochen, Germany) operated at an accelerating voltage of 20 kV equipped with EDAX. Differential scanning calorimetry (DSC) analysis was performed using a TA TG/DTA-Exstar/6300 (Seiko, Chiba, Japan) in a nitrogen atmosphere at a flow rate of 50 mL/min. The scanning temperature range was 28 to 200°C at a heating rate of 20°C/min. Tensile properties and compressive strength were evaluated using a UTM machine according to ASTM D D638 and ASTM D790, respectively.

Cytotoxicity

Samples after sterilization were preserved in 1X phosphate buffer brine (PBB) for 24 h at 37°C. New medium was used instead of MG63 cells. The cells were supplemented with SS HDPE liquid extract in triplicate, in five

T a b l e 1. Chemicals used

Name	Purpose
Disodium hydrogen phosphate Calcium nitrate tetrahydrate Ethylenediaminetetraacetic acid	Hydroxyapatite (HA) preparation using calcium apatite with the formula $Ca_5(PO_4)_3(OH)$, commonly represented as $Ca_{10}(PO_4)_6(OH)_2$
Phosphate buffer brine	A buffer solution (pH ca. 7.4) is used for biological research
MTT assay (1 Mg/Ml)	This technique is used for assessing the metabolic activity of cells as a sign of their cytotoxicity, proliferation, and viability
Organ sulfur or dimethyl sulfoxide (DMSO)	Utilized as a penetrating medium for different medications, to treat interstitial cystitis, and to cryopreserve stem cells.
Agar solution	For microbiological analysis

different volumes. After 18 h of incubation at 37±1°C, the wells were filled with MTT assay (1 mg/mL) and left to incubate for 4 h. After incubation, a small amount of organic sulfur in dimethyl sulfoxide (DMSO) was added to each well, and then a photometer was used to measure sulfur cytotoxicity at 570 nm. The cytotoxicity score (%) was calculated according to equation 2, and cell viability was calculated according to equation 3:

$$\text{Cytotoxicity} = [(\text{Control-Treated})/\text{Control}] \times 100\% \quad (2)$$

$$\text{Cell viability} = (\text{Treated}/\text{Control}) \times 100\% \quad (3)$$

The results were used to calculate cell viability and cytotoxicity [23, 24]. According to ISO 10993:5, the cytotoxicity of the HDPE/HA/zeolite composite (65/30/5) was assessed on L929 cells after 24 h.

RESULTS AND DISCUSSIONS

FT-IR analysis

FT-IR spectrum of the synthetized HA is shown in Figure 1a. The characteristic sharp band at 1051 cm^{-1} corresponds to the stretching vibrations of phosphate groups [28]. The bands at 613 cm^{-1} and 563 cm^{-1} refer to bending mode of P–O bonds in phosphate group [29]. Similarly, the weak peak at 1098 cm^{-1} indicates the symmetric stretching vibrations related to the P–O mode, confirming the presence of PO_4^{-3} group in the synthetized HA. The small peaks observed at 3658 cm^{-1} and 3584 cm^{-1} are due to O-H stretching vibrations in HA. Moreover, the weak peaks at 1426 cm^{-1} and 877 cm^{-1} are assigned to the carbonate group and clearly indicate the presence of carbonates in HA. Therefore, the obtained FT-IR spectrum confirmed the formation of HA nanoparticles, and no other impurities were identified [30–33]. FT-IR spectrum of zeolite is presented in Fig. 1b. In the hydroxyl region (4000–3000 cm^{-1}), the spectrum of zeolite showed a distinct peak at 3305 cm^{-1}, corresponding to the deformation vibrations of absorbed water. A weak peak at 1615 cm^{-1} is also related to OH stretching and deformation vibrations of adsorbed water. Other bands were observed at 902 cm^{-1} and 618 cm^{-1}. These bands can be attributed to the overlap of the asymmetric vibrations of Si-O (bridged) and $Si–O^-$ (non-bridged) bonds. The FT-IR spectrum of the HDPE/HA/zeolite composite shows characteristic peaks originating from HA and zeolite, but they differ in intensity and some of them are shifted (Fig. 1d).

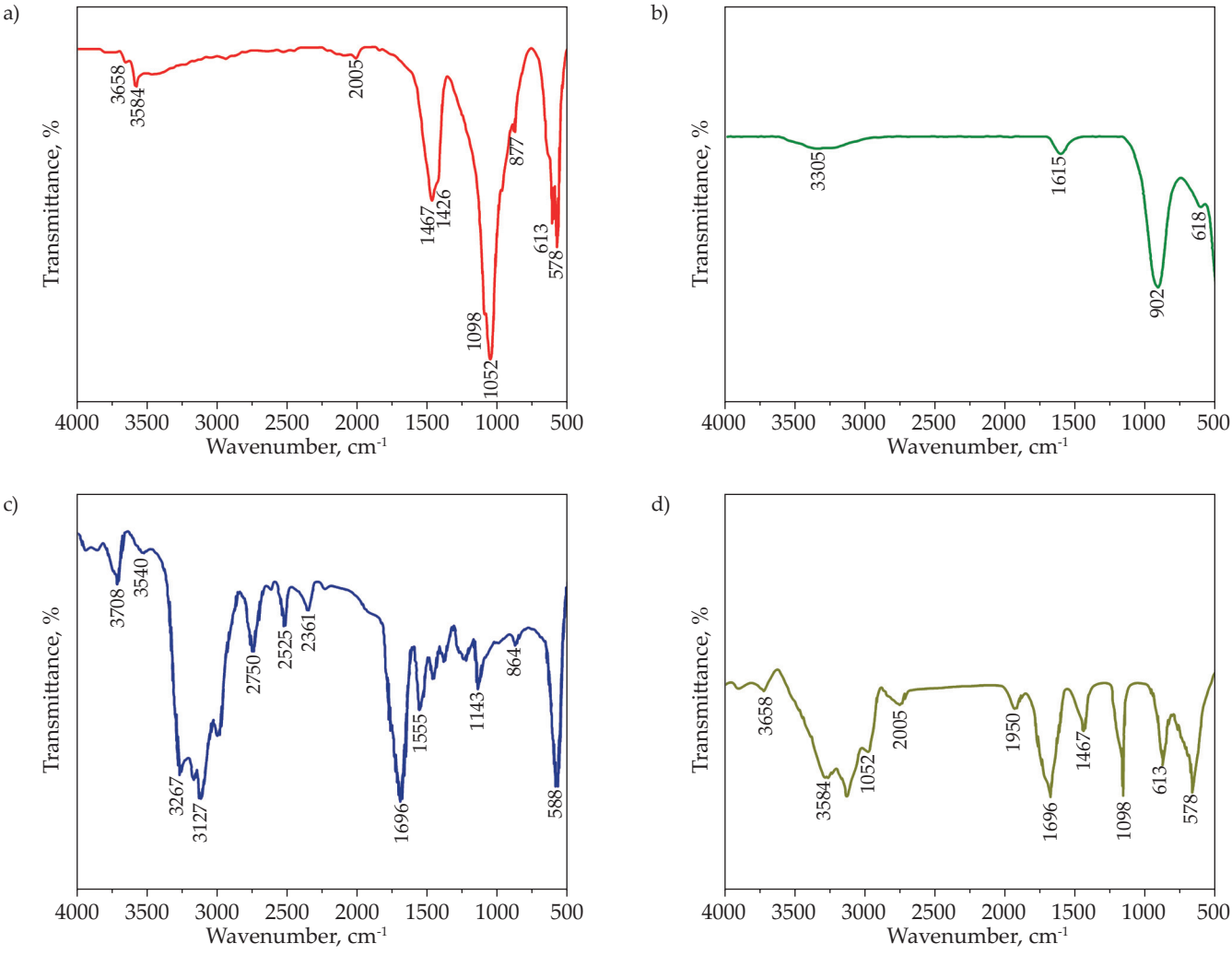

Fig. 1. FT-IR spectra: a) HA, b) zeolite, c) HDPE, d) HDPE/HA/zeolite composite

XRD analysis

The XRD patterns of HDPE, HA, zeolite, and HDPE/HA/zeolite (65/30/5) composite is shown in Fig. 2. The crystal plane orientations of the composite were found to be (131), (110), (200), (211), (202), (212), (222), and (044). The peaks caused by the zeolite reinforcement match well with the JCPDS card number 39–1380 [27, 34]. The peak at (110) is due to the orthorhombic crystal nature of polyethylene particles [35]. If the addition of HA and zeolite does not significantly disrupt the crystal structure of HDPE, the intensity of the "110 plane" peak will not decrease. If the concentration of HA and zeolite in the HDPE matrix is low, their effect on the overall crystallinity of HDPE may be negligible. This may happen if the additives are well dispersed in HDPE matrix and do not interfere with the crystallization of HDPE [36].

FESEM and EDAX analysis

The surface morphology of hydroxyapatite and HDPE/HA/zeolite composite were studied using FESEM, as shown in Fig. 3. FESEM images provide direct information on the shape and size of the synthesized HA. Fig. 3a shows the cubic morphology of the crystalline HA sample. Hydroxyapatite is a calcium phosphate compound with the chemical formula $Ca_{10}(PO_4)_6(OH)_2$. Moreover, it is known to crystallize in the hexagonal system (hexagonal symmetry). The unit cell has a hexagonal basis and is described by the lattice parameter of the basal plane (a) and the hexagonal prism. The particles resemble a tubular short wire, which was irregularly distributed with nanoparticles. Higher temperature interrupted the Ostwald ripening and capillary force and induced nucleation along the c-axis to form nanotubes [37]. Hydroxyapatite particles are usually hexagonal rod-like structures [38], which are consistent with the XRD data. Although FESEM cannot independently confirm the crystal structure, it suggests a morphology consistent with a hexagonal crystal system. The interfacial bonds between the matrix and the reinforcements are clearly visible. A similar crystallographic structure was also obtained for polyethylene/seashells composite [39, 40]. The FESEM image of the HDPE/HA/zeolite composite is shown in Fig. 3b. The hexagonal structures in the polymer matrix indicate the presence of HA particles [41]. The clean, smooth surface on the bottom of the reinforcement is derived from the HDPE polymer matrix [42].

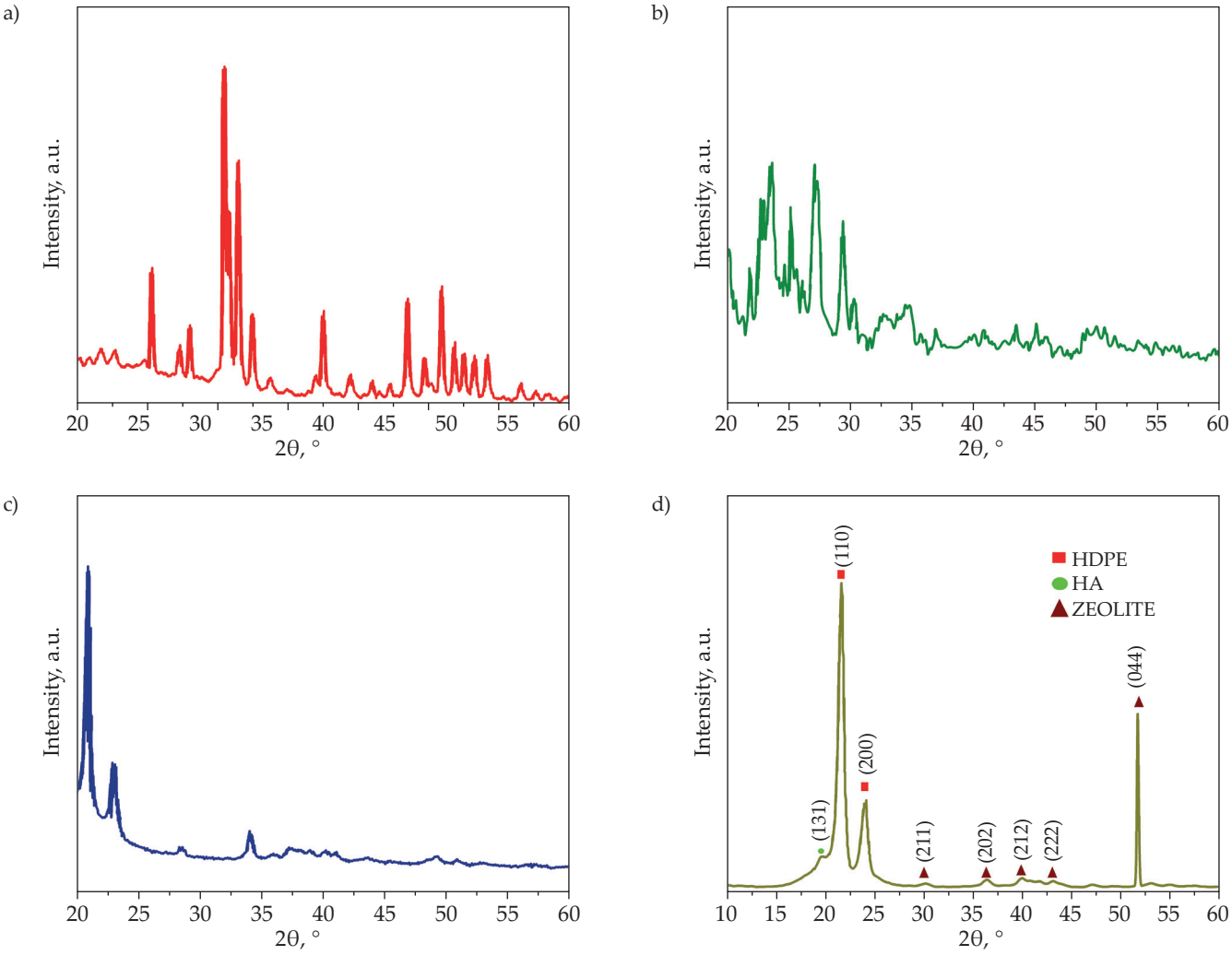

Fig. 2. XRD patterns: a) HA, b) zeolite, c) HDPE, d) HDPE/HA/zeolite composite

a) b)

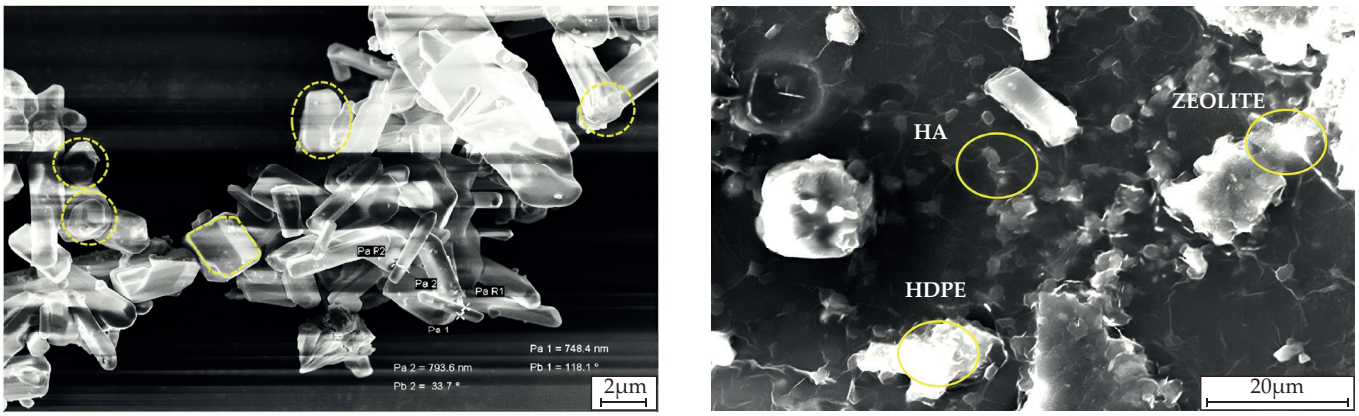

Fig. 3. FESEM images: a) HA, b) HDPE/HA/zeolite composite

EDAX pattern indicates the presence of O (63.88%), Ca (15.95%), P (7.45%), C (9.68%), Na (2.12%), Cl (0.76%), and Mg (0.17%). Oxygen and calcium are among the major elements in hydroxyapatite particles [43], while magnesium and sodium occur in trace amounts [44].

DSC analysis

Figure 4 shows DSC curve of HDPE/HA/zeolite composite. The melting temperature of the composite is 132.3°C and the energy absorption is 96.07 J/g. The results reflect the endothermic behavior of the material during heat absorption [23, 45]. In the case of endothermic processes, an increased heat flow per unit mass means that the sample requires more energy to undergo a phase change. In the case of exothermic processes, this means a greater energy release. In this analysis, a higher energy requirement to undergo a phase change may also indicate a sample with a more defined phase change or a higher concentration of the active ingredient, such as 5 wt% zeolite and 30 wt% HA [25, 46].

Mechanical properties

It is known that the addition of HA and zeolite increases the tensile strength of the material [47, 48–50]. Figure 6 shows the stress-strain curves of pure HDPE and HDPE/HA/zeolite (65/30/5) composite. It is clear from Fig. 5 that the addition of HA and zeolite to HDPE reduces the elongation at break while increasing the tensile strength from 16.3 MPa to 21.4 MPa. Moreover, the compressive strength and hardness increased from 22.5 MPa to 24.7 MPa and from 53.1 to 61 ShD, respectively (Table 2). The observed change in tensile strength is due to the use of zeolite [51]. Hydroxyapatite also increases tensile strength [52]. The increase in tensile strength may indicate a synergistic effect resulting from the simultaneous use of zeolite and hydroxyapatite. It is accepted that at high HA content, it agglomerates, restricting the molecular mobility of HDPE under stress and increasing the probability of composite failure due to external stresses. Well-dispersed fillers with good adhesion to the HDPE matrix increase tensile strength of the composite. HA and zeolite can provide reinforcement, especially if they are uniformly dispersed and have strong filler-polymer interactions. Furthermore, the dysfunctional interfacial interaction between HA and the HDPE matrix increased the formation of voids in these composites, which resulted in a poor tensile stress distribution at the filler-matrix interface. As a result, the tensile strength decreased with increasing HA filler loading. This observation is consistent with the results reported in other studies [48–50]. Filling the polymer matrix with more than one filler has been reported to increase the tensile strength [53]. Filler-polymer interactions in HDPE/HA/zeolite composites are primarily physical, involving mechanical interlocking and potentially van der Waals forces. Chemical interactions are limited due to the nonpolar nature of HDPE unless the filler is modified. These interactions significantly affect the mechanical properties of the composite and are crucial to achieving the desired properties, and often involve resolving issues related to filler dispersion and interfacial adhesion.

Biocompatibility

Biocompatibility studies were conducted to verify the compatibility of the implant with human use and to check whether the use of the implant could have potentially

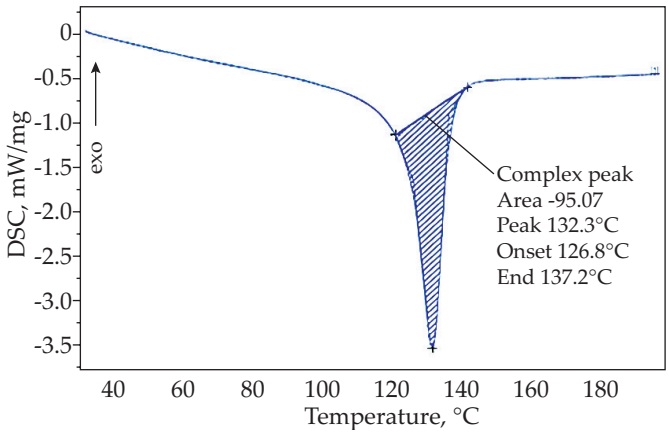

Fig. 4. DSC curve of HDPE/HA/zeolite composite

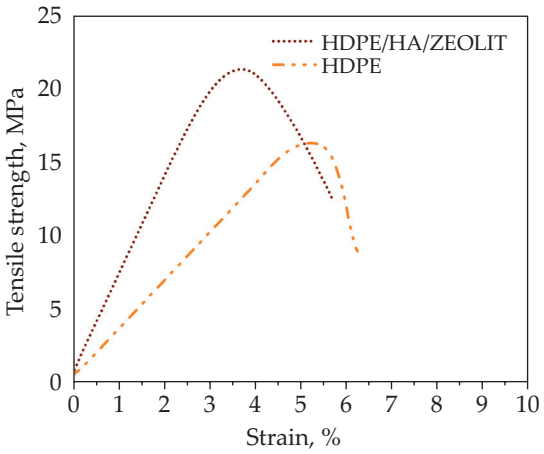

Fig. 5. Stress-strain curves of pure HDPE and HDPE/HA/zeolite composite

harmful physiological effects. *In vitro* and *in vivo* studies were conducted for various medical devices, biomaterials and related products to detect the presence of toxic or other harmful effects. The studies conducted confirmed the biocompatibility of the HDPE/HA/zeolite composite and the results obtained are consistent with other literature reports [55]. The hybrid effect of HA and zeolite may result in improved mechanical properties by combining stiffness and strength of HA with strength and barrier properties of zeolite. This combination improves bioactivity compared to the use of a single filler. The synergistic interactions between HA and zeolite in the HDPE matrix resulted in better composite properties.

Direct *in vitro* cytotoxicity

Direct *in vitro* cytotoxicity studies the harmfulness of cells cultured in the presence of an object in the same liquid medium without a barrier. The first and most important step in deciding whether to continue clinical use of a health-related product is cytotoxicity testing. ISO regulations recommend the use of uniform settings for cytotoxicity testing. Recently, several cases of blindness after simple retinal detachment surgery with PFO have been reported in Chile, Spain, and other countries. This suggests that some manufacturers' cytotoxicity results of are clinically used, PFO batches are insufficient. Most of these cases have been linked to toxic PFO batches used during procedures, according to the investigation. The procedures used to certify PFO before clinical use were unable to detect toxicity. Cellular toxicity was studied using two commonly used techniques: extract dilution and indirect contact, which uses PFO samples that are not in contact with cells [55]. In addition, the L929 cell line, which is commonly used to generate mouse fibroblasts but is more resistant to the toxicity of specific test compounds [56], was used in the study. The cytotoxicity and cell viability ratio of the HDPE/HA/zeolite (65/30/5) composite was calculated for different volumes of the extract using the direct cytotoxicity method. The calculated cytotoxicity reached 6% with a cell viability of 94%, resulting in a slight reactivity.

The HDPE/HA/zeolite composite showed little cytotoxic reactivity towards L929 cells after 24 h. Figure 6 shows the cell morphology of L929 cell line. The images revealed live and dead cells. The number of live cells is higher than the number of dead cells. This proves that biomaterial is useful in tissue engineering applications.

CONCLUSIONS

The HDPE/HA/zeolite (65/30/5) composite was obtained by injection molding. Hydroxyapatite was successfully

T a b l e 2. Mechanical properties of pure HDPE and HDPE/HA/zeolite composite

Sample	Tensile strength MPa	Compressive strength MPa	Shore hardness
Pure HDPE	16.3±0.5	22.5±0.5	53.1±0.5
HDPE/HA/zeolite	21.4±0.5	24.7±0.5	61.0±0.5

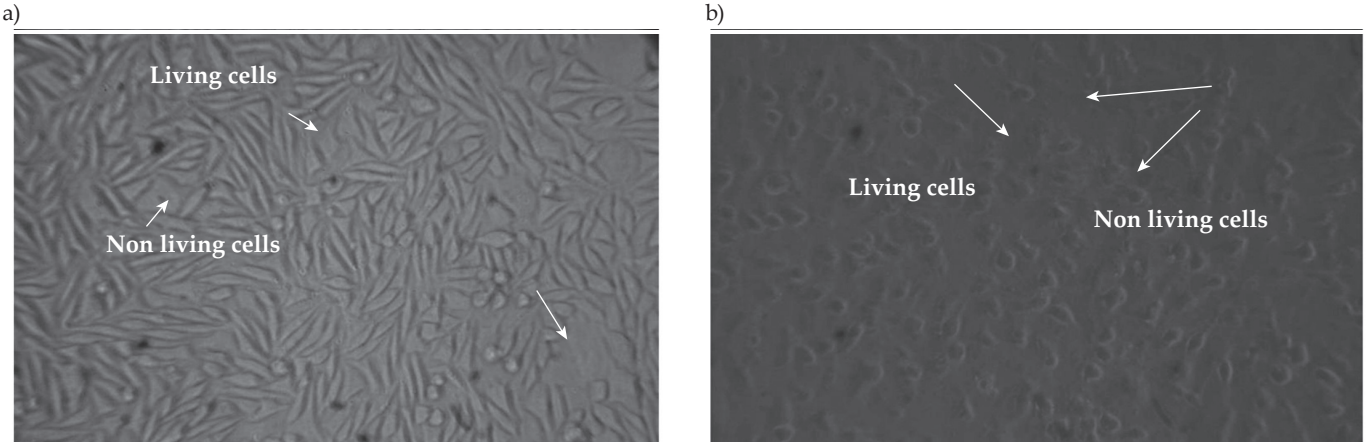

Fig. 6. Cell morphology of L929 cells: a) control, b) HDPE/HA/zeolite composite

synthetized using microwave irradiation method. FT-IR showed the presence of hydroxyl and phosphate functional groups. The crystal plane orientations such as (131), (110), (200), (211), (202), (212), (222), and (044) were determined by XRD, and the nanocrystallite size was determined to be 8.3 nm using the Debye–Scherrer equation. FESEM revealed the cubic morphology of HA. EDAX analysis showed the presence of O, Ca, P, C, Na, Cl and Mg. DSC demonstrated that the melting point of the composite was higher than the melting point of pure HDPE. Moreover, the composite had improved tensile strength, compressive strength, and hardness. *In vitro* cytotoxicity studies were conducted using L929 cell line. The tests showed 94% viability and 6% toxicity of cells. The results showed that the HDPE/HA/zeolite composite is a promising candidate for medical applications, e.g., in implants.

Authors contribution

A.M.A. – conceptualization, investigation, validation, writing-original draft, writing-review and editing, visualization; S.K. – writing-review and editing; M.S. – data collection, investigation, validation, writing-original draft; B.A.C. – writing-review and editing; S.K.K.L. – writing-review and editing.

Funding

Self and no external funding involved in this research work.

Conflict of interest

The authors declare no conflict of interest.

REFERENCES

[1] Piveteau L.D., Girona M.I., Schlapbach L. *et al*.: *Journal of Material Science: Materials in Medicine* **1999**, *10*, 161. https://doi.org/10.1023/A:1008985423644

[2] Long M., Rack H.J.: *Biomaterials* **1998**, *19(18)*, 1621. https://doi.org/10.1016/S0142-9612(97)00146-4

[3] Williams D.F.: *Sadhana* **2003**, *28*, 563. https://doi.org/10.1007/BF02706447

[4] Tang. Y.C., Katsuma S., Fujimoto S. *et al*.: *Acta Biomaterialia* **2006**, *2(6)*, 709. https://doi.org/10.1016/j.actbio.2006.06.003

[5] Okazaki Y., Gotoh E., Manabe T *et al*.: *Biomaterials* **2004**, *25(58)*, 5913. https://doi.org/10.1016/j.biomaterials.2004.01.064

[6] Kannan S., Balamurugan A., Rajeswari S.: *Electrochimica Acta* **2004**, *49(15)*, 2395. https://doi.org/10.1016/j.electacta.2004.01.003

[7] Kannan S., Balamurugan A., Rajeswari S.: *Electrochimica Acta* **2005**, *50(15)*, 2065. https://doi.org/10.1016/j.electacta.2004.09.015

[8] Prabakaran K., Rajeswari S.: *Journal of Applied Electrochemistry* **2009**, *39*, 887. https://doi.org/10.1007/s10800-008-9738-5

[9] Gopi D., Collins Arun Prakash V., Kavitha L. *et al*.: *Corrosion Science* **2011**, *53(6)*, 2328. https://doi.org/10.1016/j.corsci.2011.03.018

[10] Shi C., Yuan Z., Han F. *et al*.: *Annals of Joint* **2016**, *1(9)*, 27. https://doi.org/10.21037/aoj.2016.11.02

[11] Ito A., Otsuka M., Kawamura H. *et al*.: *Current Applied Physics* **2005**, *5(5)*, 402. https://doi.org/10.1016/j.cap.2004.10.006

[12] Rossi L., Migliaccio S, Corsi A. *et al*.: *The Journal of Nutrition* **2001**, *131(4)*, 1142. https://doi.org/10.1093/jn/131.4.1142

[13] Moonga B.S., Dempster D.W.: *Journal of Bone and Mineral Research* **1995**, *10(3)*, 453. https://doi.org/10.1002/jbmr.5650100317

[14] Yamaguchi M., Oishi H., Suketa Y.: *Bochemical Pharmacology* **1987**, *36(22)*, 4007. https://doi.org/10.1016/0006-2952(87)90471-0

[15] Ito A., Kawamura H., Otsuka M. *et al*.: *Material Science and Engineering: C* **2002**, *22(1)*, 21. https://doi.org/10.1016/S0928-4931(02)00108-X

[16] Ito A., Ojima K., Naito H. *et al*.: *Journal of Biomedical Materials Research* **2000**, *50(5)*, 178. https://doi.org/10.1002/(SICI)1097-4636(200005)50:2<178:AID-JBM12>3.0.CO;2-5

[17] Rossi L., Migliaccio S., Corsi A. *et al*.: *The Journal of Nutrition* **2001**, *131(4)*, 1142. https://doi.org/10.1093/jn/131.4.1142

[18] Uysal I., Severcan F., Tezcaner A. *et al*.: *Progress in Natural Science: Materials International* **2014**, *24(4)*, 340. https://doi.org/10.1016/j.pnsc.2014.06.004

[19] Cacciotti I., Bianco A., Lombardi M. *et al*.: *Journal of the European Ceramic Society* **2009**, *29(14)*, 2969. https://doi.org/10.1016/j.jeurceramsoc.2009.04.038

[20] Ciftci F., Özarslan A.C.: *Nanostructures and Nano-Objects* **2024**, *38*, 101152. https://doi.org/10.1016/j.nanoso.2024.101152

[21] Yilmaz B., Alshemary A.Z., Evis Z.: *Microchemical Journal* **2019**, *144*, 443. https://doi.org/10.1016/j.microc.2018.10.007

[22] Harun W.S.W., Asri R.I.M., Alias J. *et al*.: *Ceramics International* **2018**, *44(2)*, 1250. https://doi.org/10.1016/j.ceramint.2017.10.162

[23] Balaji Ayyanar C., Marimuthu K.: *Polymers and Polymer Composites* **2019**, *28(4)*, 285. https://doi.org/10.1177/0967391119872877

[24] Balaji Ayyanar C., Marimuthu K., Gayathri B. *et al*.: *Polymers and Polymer Composites* **2021**, *29(9)*, 1534. https://doi.org/10.1177/0967391120981551

[25] Udhayakumar G., Muthukumarasamamy N., Velauthapillai D. *et al.*: *Applied Physics A* **2017**, *123*, 655. https://doi.org/10.1007/s00339-017-1248-z
[26] Gayathri B., Muthukumarasamy N., Velauthapillai D. *et al.*: *Arabian Journal of Chemistry* **2018**, *11(5)*, 645. https://doi.org/10.1016/j.arabjc.2016.05.010
[27] Kashkarov V.M., Goloshchapov D.L. Rumyantseva A.N. *et al.*: *Journal of Surface Investigation. X-ray, Synchrotron and Neutron Techniques* **2011**, *5*, 1162. https://doi.org/10.1134/s1027451011120068
[28] Ramanan S.R., Venkatesh R.: *Materials Letters* **2004**, *58(26)*, 3320. https://doi.org/10.1016/j.matlet.2004.06.030
[29] Russell S.W., Luptak K.A., Tres C.A. *et al.*: *Journal of the American Ceramic Society* **1996**, *79(4)*, 837. https://doi.org/10.1111/j.1151-2916.1996.tb08514.x
[30] Markovic M., Fowler B.O. Tung M.S: *Journal of Research of the National Institute of Standards and Technology* **2004**, *109*(*6*), 553. https://doi.org/10.6028/jres.109.042
[31] Głąb M., Kudłacik–Kramarczyk S., Drabczyk A. *et al.*: *Molecules* **2021**, *26*(*14*), 4268. https://doi.org/10.3390/molecules26144268
[32] Sari M., Yusuf Y.: *IOP Conference Series: Materials Science and Engineering* **2018**, *432*, 012046. https://doi.org/10.1088/1757-899x/432/1/012046
[33] Wijiyanti R., Kumala Wardhani A.R., Roslan R.A. *et al.*: *Malaysian Journal of Fundamental and Applied Sciences* **2020**, *16*(2), 128. https://doi.org/10.11113/mjfas.v16n2.1472
[34] Wu X., Peng L., Xu Y. *et al.*: *RSC Advances* **2018**, *8*(*40*), 22583. https://doi.org/10.1039/c8ra03366h
[35] Burton A.W., Ong K., Rea T. *et al.: Microporous and Mesoporous Materials* **2009**, *117*(*1-2*), 75. https://doi.org/10.1016/j.micromeso.2008.06.010
[36] Thomas P.S., Thomas S., Bandyopadhyay S. *et al.*: *Composites Science and Technology* **2008**, *68*(15-16), 3220. https://doi.org/10.1016/j.compscitech.2008.08.008
[37] Mondal S., Dorozhkin S.V., Pal U.: *Nanomedicine and Nanobiotechnology* **2017**, *10(4)*, e1504. https://doi.org/10.1002/wnan.1504
[38] Jaggi H.S., Kumar Y., Satapathy B.K. *et al.*: *Materials and Design* **2012**, *36*, 757. https://doi.org/10.1016/j.matdes.2011.12.004
[39] Turkez H., Yousef M.I., Sönmez E. *et al.*: *Journal of Applied Toxicology* **2013**, *34*(4), 373. https://doi.org/10.1002/jat.2958
[40] Price L.A., Ridley C.J., Bull C.L. *et al.*: *CrystEngComm* **2021**, *23*(*33*), 5615. https://doi.org/10.1039/D1CE00142F
[41] Khalid H.U., Ismail M.C., Nosbi N.: *Materials* **2021**, *14*(11), 2823. https://doi.org/10.3390/ma14112823
[42] Sun W., Chu C., Wang J. *et al.*: *Journal of Materials Science: Materials in Medicine* **2006**, *18*(5), 677. https://doi.org/10.1007/s10856-006-0019-8
[43] Abifarin J.K., Obada D.O., Dauda E.T. *et al.*: *Data in Brief* **2019**, *26*, 104485. https://doi.org/10.1016/j.dib.2019.104485
[44] Passador F.R., Ruvolo A.C., Pessan L.A.: *Polimeros* **2012**, *22*(4), 357. https://doi.org/10.1590/s0104-14282012005000052
[45] https://www.shimadzu.com/an/industries/environment/microplastics/measuring-polyethylene/index.html
[46] Safandowska M., Makarewicz C., Różański A. *et al.*: *Scientific Reports* **2023**, *13*, 19838. https://doi.org/10.1038/s41598-023-46276-9
[47] Souza A.F, Behrenchsen L., Souza S.J. *et al.*: *International Food Research Journal* **2018**, *25*(3), 1309.
[48] Lim K.L.K., Ishak Z.M., Ishiaku U.S. *et al.*: Journal of Applied Polymer Science **2006**, *100(5)*, 3931. https://doi.org/10.1002/app.22866
[49] Liu T., Huang K., Li L. *et al.*: Composites Science and Technology **2019**, *175*, 100. https://doi.org/10.1016/j.compscitech.2019.03.012
[50] Abdel Rahman RO., Zaki A.A., El-Kamash A.M.: *Journal of Hazardous Materials* **2007**, *145*(3), 372. https://doi.org/10.1016/j.jhazmat.2006.11.030
[51] Al-Sanabani J.S., Madfa A.A., Al-Sanabani F.A.: *International Journal of Biomaterials* **2013**, *1*, 876132. https://doi.org/10.1155/2013/876132
[52] Mustaffa N.A.: "Nano Alumina Radiation Effect on Thermo-mechanical Properties of High-Density Polyethylene-hydroxyapatite Composite", Ph.D. Thesis, Universiti Putra Malaysia, Serdang 2021.
[53] Shah K.S., Jain R.C., Shinet V. *et al.*: *IEEE Transactions on Dielectrics and Electrical Insulation* **2009**, *16*(3), 853. https://doi.org/10.1109/tdei.2009.5128526
[54] Pastor J.C., Coco R.M., Fernandez-Bueno I. *et al.*: *Retina* **2017**, *37(6)*, 1140. https://doi.org/10.1097/IAE.0000000000001680
[55] Wen X., Wang R., Jia X. *et al.*: *Chinese Journal of Medicinal Instrumentation* **2015**, *39*(*3*), 212.
[56] Moorthy A.A., Nanjappan N., Ayyanar C.B. *et al.*: *Journal of Engineering Research – ICMMM Special Issue* **2021**. https://doi.org/10.36909/jer.ICMMM.12431

Received 26 IV 2024.
Accepted 14VIII 2024.